



# High-frequency characterization of magnetic permeability using extended single-turn inductor and microstrip methods

Saulius Rudys<sup>a,d</sup>, Christine Vollinger<sup>b</sup>, Liudas Tumonis<sup>c</sup>, Juras Banyas<sup>d</sup>, Vidmantas Kalendra<sup>d,\*</sup>

<sup>a</sup> Antanas Gustaitis' Aviation Institute, Vilnius Gediminas Technical University, Linkmenų Str. 28-4, Vilnius 08217, Lithuania

<sup>b</sup> CERN, Geneva, Switzerland

<sup>c</sup> Institute of Chemical Physics, Vilnius University, Sauletekio Ave. 3, Vilnius 10257, Lithuania

<sup>d</sup> Institute of Applied Electrodynamics and Telecommunications, Vilnius University, Sauletekio Ave. 3, Vilnius 10257, Lithuania

## ARTICLE INFO

### Keywords:

Ferrites  
Magnetic permeability  
Microstrip line  
Single-turn inductor

## ABSTRACT

The presence of anisotropy in the properties of materials presents challenges for their characterization. This is particularly relevant for magnetic materials, which are often sensitive to external fields. As such, the characterization of magnetic materials is a complex task. In this study, we propose extending the frequency range of the classic single-turn inductor method for disc-shaped samples with holes into the GHz range, utilizing numerical methods provided by Ansoft HFSS software. The measurement of the components of the magnetic permeability tensor depends on the direction of the applied magnetic field. To change the magnetic field direction, we developed a microstrip measurement setup for the same disc-shaped sample. Due to the complexity of the underlying mathematical model, we employed numerical methods to calculate the magnetic permeability.

## 1. Introduction

A wide range of magnetic materials, including ferrites, magneto-dielectrics, and multiferroics, are utilized in various applications. Among these, ferrites are the most widely used due to their high magnetic permeability. This property makes ferrites suitable for a broad spectrum of uses, from conventional electronic equipment to high-performance applications, such as fast kicker magnets in injection and extraction systems of circular accelerators [1,2]. The magnetic properties of ferrites are highly frequency-dependent [3], with typical radio frequency responses exhibiting at least two distinct processes across a wide frequency range [4]. Furthermore, the magnetic permeability of ferrites is sensitive to the external magnetic field. When an external field is applied, an initially isotropic material becomes anisotropic, and its magnetic permeability transitions from a scalar to a tensor.

However, ferrite manufacturers typically provide only basic data, which is insufficient for accurately determining the frequency dependence of magnetic permeability or its variation with the external field—information crucial for many applications. Tsutaoka et al. demonstrated a method for recovering the magnetic permeability dependence on frequency using manufacturer-provided parameters, along with experimental data [4]. Our analysis reveals discrepancies between the recovered curves, which can be significant for certain

practical applications, such as beam coupling impedance simulations in particle accelerators. Thus, precise measurements of ferrites are essential for optimizing their performance in these applications.

## 2. Measurement methods

The measurement of the electromagnetic properties of materials involves three main components: measurement equipment, the device under test (DUT) containing the investigated material, and a mathematical model. The model establishes the relationship between the electrical values measured by the equipment and the physical properties of the material, which is the ultimate goal of the measurement. For instance, by measuring the complex reflection coefficient of a DUT using a vector network analyzer, it is possible to calculate magnetic permeability using a corresponding mathematical model. Various DUT configurations for measuring dielectric permittivity and magnetic permeability are shown in Fig. 1. Note that DUT configurations for high-quality-factor materials are not included in Fig. 1. The mathematical model is straightforward in only a few cases, such as: a thin capacitor with a dielectric between the plates (Fig. 1a); a single-turn inductor with disc-shaped samples featuring a central hole (Fig. 1h); a transmission line in dielectric and magnetic media (Fig. 1b and 1c). The sensitivity of the measurement system to the electric or magnetic properties depends

\* Corresponding author.

E-mail address: [vidmantas.kalendra@ff.vu.lt](mailto:vidmantas.kalendra@ff.vu.lt) (V. Kalendra).

<https://doi.org/10.1016/j.jmmm.2025.173214>

Received 3 March 2025; Received in revised form 5 May 2025; Accepted 20 May 2025

Available online 21 May 2025

0304-8853/© 2025 The Author(s). Published by Elsevier B.V. This is an open access article under the CC BY license (<http://creativecommons.org/licenses/by/4.0/>).

on the field strength within the sample. For example: case (a) is most suitable for dielectric permittivity measurements since the sample is located in a region with maximum electric and minimal magnetic fields; case (h) is ideal for magnetic permeability measurements for a similar reason. When both magnetic permeability and dielectric permittivity need to be measured, a two-port DUT and a vector network analyzer (VNA) are required.

The main properties of the DUTs are presented in Fig. 1 and are described below:

- a) **Serial Capacitor Method:** This method is analyzed using a very simple mathematical model [5]. Even when magnetic permeability is present, the method allows dielectric permittivity measurements using a one-port DUT with a conductive plane behind the sample. However, when the dielectric permittivity or frequency is high, the electric field in the sample becomes non-uniform, necessitating a more complex mathematical model [6,7].
- b) **Serial Ring Method:** This method assumes a transverse electromagnetic (TEM) wave propagation and is described by a simple mathematical model [8]. It is suitable for simultaneous measurements of magnetic permeability and dielectric permittivity. Magnetic field lines are circular within the sample, which limits the ability to measure the magnetic permeability tensor. The main drawbacks are the need for precise fabrication of the sample and electrical contact with the inner and outer coaxial conductors.
- c) **Full-Filled Rectangular Waveguide:** This method, analyzed with a simple mathematical model [9], features circular magnetic field lines in the horizontal plane, limiting its ability to measure the magnetic permeability tensor. It is unsuitable for high dielectric permittivity measurements (e.g., in the tens to hundreds range) due to excessive reflection from the sample.
- d) **Rod in Rectangular Waveguide:** This method involves a complex mathematical model. Models have been developed for samples with circular and rectangular cross-sections [5]. The sample is placed at the center of the waveguide, where the electric field is maximum.

- e) **Free-Space Method:** The analysis of this method can be described by a simple mathematical model [10]. In open space, the electric (E) and magnetic (B) field lines are nearly straight, making this method suitable for measuring the magnetic permeability tensor. However, the major limitation is the large size required for the sample.
- f) **Microstrip Line Method:** This method uses a complex mathematical model, and parasitic effects from the connecting elements and port coupling can influence measurement precision. To account for these effects, numerical methods are essential [11]. Both magnetic permeability and dielectric permittivity can be measured using a two-port configuration. As the E and H field lines are nearly straight within the sample, this method is well-suited for measuring the magnetic permeability tensor. An advantage of this method is that it requires only a small sample.
- g) **Open-Ended Coaxial Line Method:** This method is described by a complex mathematical model [12–16]. It is well-suited for measuring the dielectric permittivity of liquids [12] and requires good electrical contact and precise manufacturing of the coaxial line. Measurements can be performed over a wide frequency range (up to three orders of magnitude) and at high frequencies (up to tens of GHz).
- h) **Single-Turn Inductor Method:** This method is based on a simple mathematical model [17]. It is one of the most popular methods for measuring magnetic permeability at GHz frequencies. A key advantage of this method is that no electrical contact with the sample is required, allowing the same DUT to be used for multiple samples. The calibration of the measurement setup is straightforward. However, the magnetic field lines are circular within the sample, limiting the ability to measure the magnetic permeability tensor.

In this paper, we focus on the single-turn inductor and microstrip line methods.

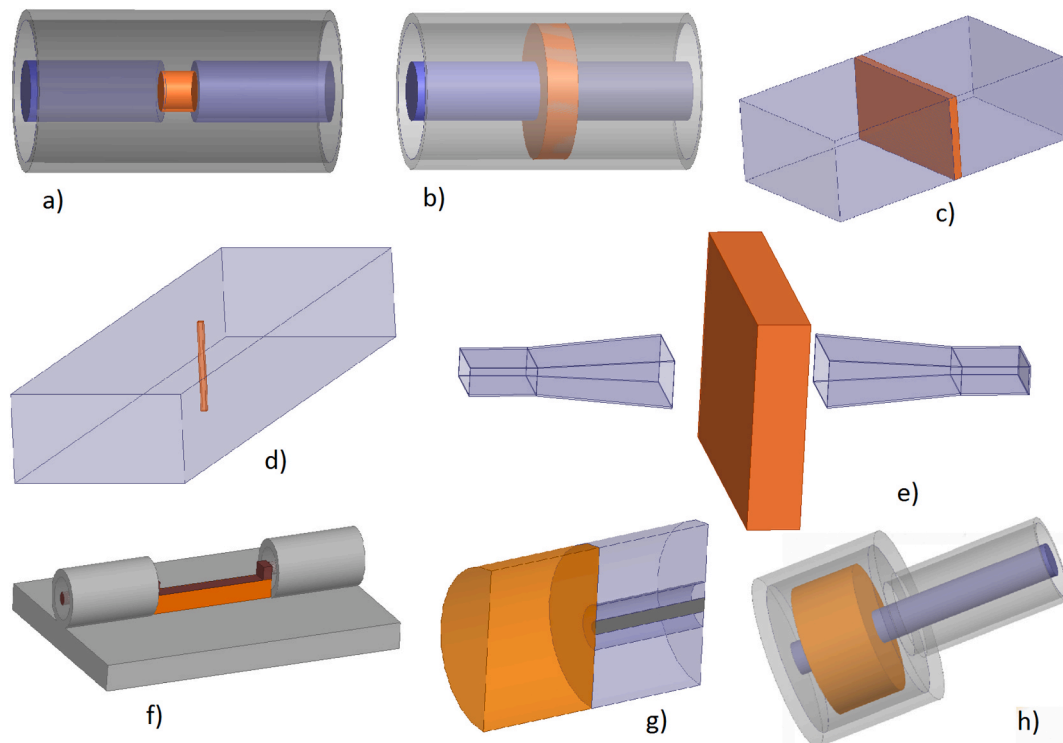


**Fig. 1.** Different methods for measuring the dielectric permittivity and magnetic permeability of DUTs: (a) serial capacitor, (b) serial ring, (c) fully-filled rectangular waveguide, (d) rod in a rectangular waveguide, (e) free-space method, (f) microstrip line, (g) open-ended coaxial line, and (h) single-turn inductor.

The extraction of magnetic permeability using simulation involves solving an inverse problem: determining unknown material parameters (permittivity and permeability) from known S-parameters measured experimentally. We employed Ansoft HFSS software's optimization tools to address this problem. First, the sample and DUT geometries were precisely modeled in 3D. Simulations were then performed with initial guesses for electromagnetic properties of the material. The software iteratively adjusts the values of magnetic permeability and dielectric permittivity to minimize the error between measured and simulated S-parameters. This process involves various optimization algorithms (we used Newton optimization) built into HFSS, which continues until the simulated response closely matches experimental measurements.

This approach (in more detail is presented in [11]) requires full calibration of the VNA and detailed knowledge of the DUT geometry and material interfaces. As a result, each simulation point requires significant computational time (from a few to tens of minutes), depending on frequency and complexity. For both the single-turn inductor and microstrip setups, we used this inverse technique to extract the real and imaginary parts of magnetic permeability.

### 3. Single-turn inductor

#### 3.1. Measurement setup

The single-turn inductor-based measurement method for magnetic permeability is one of the most widely used techniques due to its simple mathematical model, hardware design, and straightforward calibration. A shorted coaxial cavity can be considered a single-turn inductor with axial symmetry, as shown in Fig. 1h). The mathematical model is represented by the following equation (1) [17], where the complex magnetic permeability is directly expressed:

$$\mu = \frac{(Z_m - Z_{sm})2\pi}{j\omega\mu_0 h \ln \frac{c}{b}} + 1 \quad (1)$$

here  $\mu$  – relative permeability,  $Z_m$  – measured impedance with toroidal core,  $Z_{sm}$  – measured impedance without toroidal core,  $\mu_0$  – permeability of free space,  $h$  – height of the sample,  $c$  – outer diameter of the sample, and  $b$  – inner diameter of the sample. It is important to note that the magnetic permeability is independent of the cavity dimensions, and there is no requirement for electric contact with the sample. Consequently, the same DUT can be used to measure samples with varying dimensions. To determine the magnetic permeability, we measure the impedance of the empty cavity ( $Z_{sm}$ , which serves as the calibration reference) and the impedance of the cavity with the toroidal sample ( $Z_m$ ). Full calibration of the measurement port is not necessary. Despite (1) equation containing  $h$  which is the length of transmission line, this equation is related to lumped circuits, rather than transmission lines. The meaning of denominator is an impedance (inductive). Inductance  $\mu_0 h \ln \frac{c}{b}$  is proportional to the length  $h$ .

The distribution of the magnetic field strength within the sample is illustrated in Fig. 2. The field distribution is simulated using Ansoft HFSS software, which supports material anisotropy but does not account for nonlinearity. It is assumed that the devices operate in a linear regime, regardless of input power or the strength of the magnetic fields.

Since the magnetic field lines within the sample are circular, this setup allows us to measure the components of the magnetic permeability tensor, which are equal and aligned parallel to the sample plane.

The measurement setup, utilizing a standard 7/8" coaxial line, was fabricated as shown in Fig. 3. The DUT consists of a 7/8" flange cover with a cavity to hold the sample and central conductor. The RF connector is made from brass, with the outer and inner conductors being silver-plated, and the external ring is nickel-plated. The outer conductor of the sample holder (DUT) is made from aluminum, while the inner conductor is constructed from gold-plated brass. To enhance the low-frequency response, the sample was fabricated to fill the maximum

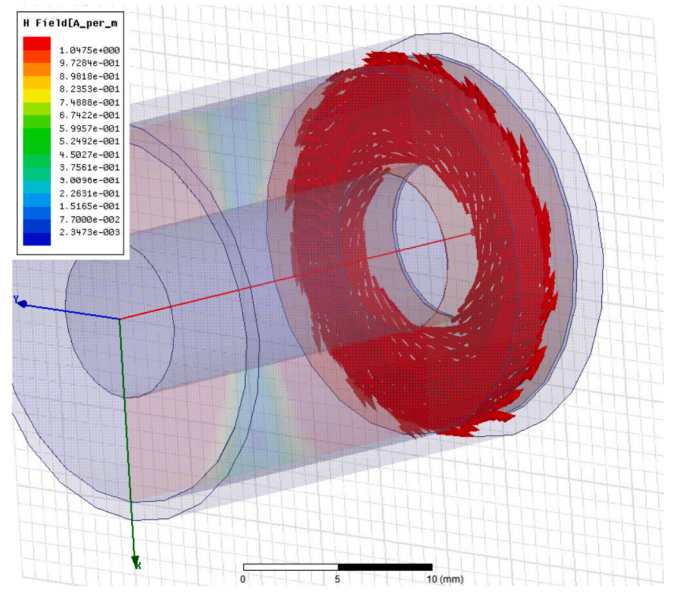


Fig. 2. Typical magnetic field strength distribution in the ferrite sample. The input power is set to 1 W, and the RF source impedance is 50  $\Omega$ . The magnetic field strength is represented on the color scale bar displayed on the left side of the figure.



Fig. 3. Measurement setup using single-turn inductor method for AL-800 ferrite, with a standard 7/8 coaxial line.

volume of the cavity. The DUT dimensions were carefully chosen to be as close as possible to the sample dimensions, with a tolerance of just 0.2 mm larger. Measurements were conducted using a Hewlett-Packard 8753E VNA.



### 3.2. Experimental results

First, we measured the impedance ( $Z_m$ ) of the ferrite AL-800 [18] in the frequency range from 1 MHz to 5.5 GHz. The magnetic permeability was calculated using equation (1). The frequency dependence of the magnetic permeability is shown in Fig. 4, demonstrating the typical behavior of ferrites, where two processes are attributed to spin and domain wall contributions. Additionally, a third process is observed in the frequency range up to 2 GHz. At frequencies higher than 2 GHz, a resonance-like behavior in magnetic permeability is evident. This sharp increase in permeability at higher frequencies lacks a clear physical explanation. Consequently, we suspect that the lumped inductor model is not valid at these higher frequencies, where the sample dimensions are comparable to the wavelength. In this regime, the sample should be treated not as a lumped inductor but as a transmission line, as illustrated in Fig. 1b). From the input impedance of a transmission line equation follows, that if we increase shorted line length from zero to quarter wave, then input impedance goes high from zero to infinity. Qualitatively it responds to an increase in the real part of magnetic permeability at high frequencies in Fig. 4. However, our case is more complex than the typical transmission line scenario, as factors such as the gaps between conductors, the dimensions of the DUT, and the dielectric permittivity of the sample must also be considered. Therefore, the mathematical model becomes significantly more complex.

To simulate these complex structures, numerical methods are required. Commercial software based on various numerical solutions to Maxwell's equations has emerged, allowing for electromagnetic (EM) simulations of intricate 3D structures. For example, the software can calculate the scattering parameters (S-parameters) of a device when the dimensions, shape, and electrical properties of the material are known. However, in the case of dielectric property measurements, the reverse problem must be solved: finding the material's electrical properties from the measured S-parameters. Unfortunately, most of these EM simulation tools are not optimized for this inverse task.

Some EM simulation software packages offer optimization features. This means that if the goal is to match S-parameters, the software can adjust the device's dimensions and/or electromagnetic properties (in our case, the electrical properties of the sample, which is part of the DUT). We adopted this approach, as presented in [11], by using Ansoft HFSS software. To ensure accurate S-parameters, a full one-port

calibration was performed.

The calculated magnetic permeability results are presented in Fig. 4 as blue and green dots, overlaid on the corresponding curves of magnetic permeability obtained using the single-turn inductor method. While the resonance behavior of the permeability curves is evident at frequencies above 2 GHz, the resonance frequency is either at or above 5 GHz (the wavelength at 5 GHz is 60 mm, and the quarter-wavelength is 15 mm). The dielectric permittivity of the sample was previously measured to be 16 [19]. With a sample thickness of 4 mm, the electrical length of the sample is calculated as  $4 \text{ mm} \times \sqrt{16} = 16 \text{ mm}$ , which is close to the quarter-wavelength (15 mm) in free space, or in a transmission line without dispersion or dielectric/magnetic media. This suggests that the sample behaves as a quarter-wavelength resonator.

Due to the computational time required (on the order of minutes to tens of minutes per calculation point), we chose to calculate fewer points than those predicted by equation (1). Nonetheless, a good agreement between the two methods was achieved. Rather than showing sharp resonance-like curves, the results show the real part of the dielectric permittivity close to unity and the imaginary part near zero at frequencies above 3 GHz, which are physically plausible results.

## 4. Microstrip method

### 4.1. Measurement setup

A microstrip line can serve as the device under test (DUT) for measuring electromagnetic properties [11]. In this setup, a transverse electromagnetic (TEM) wave propagates through the sample. Unlike circular magnetic fields, the field lines in this configuration are straight, parallel to the strip, and perpendicular to the propagation direction. This makes a microstrip DUT particularly suitable for measuring the magnetic permeability tensor. By connecting the microstrip to a two-port vector network analyzer (VNA), both electric and magnetic properties can be effectively characterized.

In practice, the field distribution in the DUT is more complex. Parasitic effects, such as those arising from the coaxial-to-microstrip transition and inter-port coupling, must be considered. At higher frequencies or when the magnetic permeability and dielectric permittivity are high, a longitudinal component of the magnetic field may also arise [11]. This introduces additional complexity to the mathematical modeling.

To address these challenges, we propose using the same toroidal sample employed in the single-turn inductor method for the microstrip measurement setup. However, this approach further complicates the mathematical model, necessitating the use of numerical methods for analysis.

The DUT structure and simulated field distribution are illustrated in Fig. 5. As anticipated, the magnetic field strength lines in the sample are straight, parallel to the strip, and perpendicular to the direction of propagation. For enhanced accuracy, a full two-port calibration was performed. Magnetic permeability calculations were based on averaged pairs of  $S_{11}$ ,  $S_{22}$  and  $S_{12}$ ,  $S_{21}$  data.

### 4.2. Experimental results

The experimental results for magnetic permeability measurements using a microstrip DUT with an AL-800 ferrite sample are shown in Fig. 6. These results are represented as blue and green dots plotted alongside the reference curves (dark blue and red), which were obtained using the single-turn inductor method. The agreement between the microstrip measurements and the single-turn inductor method is less consistent at lower frequencies compared to the experimental results in Fig. 4 from the previous chapter. This reduced accuracy at low frequencies can be attributed to the smaller sample volume (approximately three times smaller) exposed to the magnetic field in the microstrip setup.

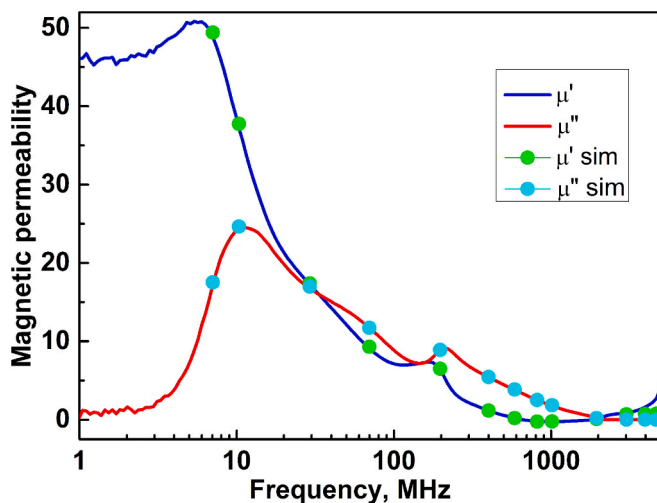


Fig. 4. Frequency dependence of the real ( $\mu'$ ) and imaginary ( $\mu''$ ) parts of magnetic permeability of AL-800 ferrite using a single-turn inductor method. Blue and green dots indicate the calculated values using the Ansoft HFSS EM simulation software. Measurements were performed at room temperature. (For interpretation of the references to color in this figure legend, the reader is referred to the web version of this article.)

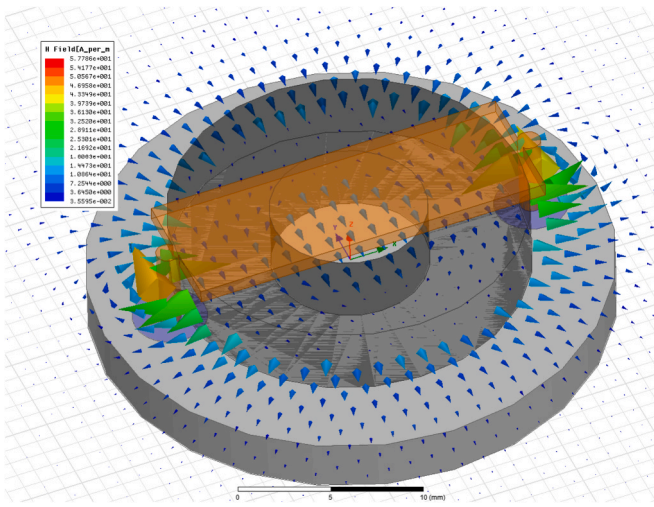


Fig. 5. Simulation of the magnetic field distribution in the microstrip DUT with of AL-800 ferrite at 100 MHz frequency. Parameters used for simulation:  $\mu'=7$ ,  $\mu''=7$ ,  $\epsilon'=17$ ,  $\epsilon''=0.01$ .

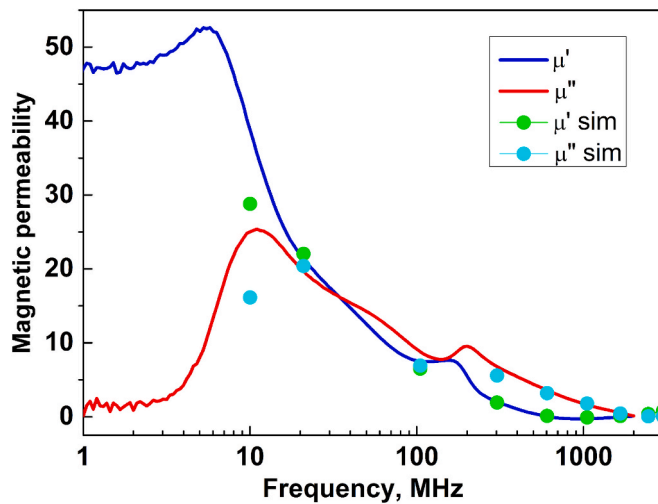
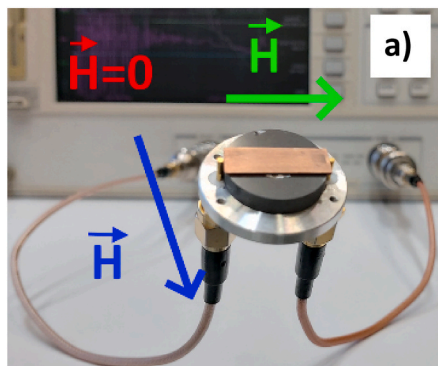


Fig. 6. Frequency dependence of the real ( $\mu'$ ) and imaginary ( $\mu''$ ) parts of magnetic permeability of AL-800 ferrite using a single-turn inductor setup. Blue and green dots indicate the calculated values using the Ansoft HFSS EM simulation software on microstrip setup. Measurements were performed at room temperature. (For interpretation of the references to color in this figure legend, the reader is referred to the web version of this article.)



Due to the complexity of the microstrip model, the calculations for each data point were significantly more time-consuming than those for the single-turn inductor, requiring tens of minutes per point.

Although the sample tested was isotropic without an external field, the microstrip setup can measure different components of the magnetic permeability tensor by simply rotating an anisotropic sample. Anisotropy in magnetic permeability can also be induced in ceramics by applying an external magnetic field. While measuring the complete tensor of magnetic permeability was not the focus of this study, the microstrip method shows potential for such applications.

To simplify the analysis and avoid the time-consuming calculations of magnetic permeability, the group delay parameter can be used as an alternative. Group delay, which is directly measurable using a VNA, is correlated to the real parts of both magnetic permeability and dielectric permittivity. Fig. 7 demonstrates that group delay exhibits different behaviors under varying magnetic fields, suggesting that it can provide insights into the magnetic permeability tensor.

At low frequencies, the reflection coefficient (for the single-turn inductor) or transmission coefficient (for the microstrip) approaches unity. This is because the small sample size leads to negligible impedance changes in the DUT for both methods. As a result, the accuracy of the measurements depends on the uncertainty of the analyzer near high reflection or transmission values.

Due to the negligible (and often unmeasurable) change in input impedance compared to a similar strip line, performing measurements and calculations using software optimization functions is impractical at low frequencies. A rough uncertainty estimation was carried out for both methods. For the single-turn inductor method:  $\pm 5\%$  below 2 GHz, increasing to  $\pm 10\%$  above 3 GHz. For the microstrip method:  $\pm 10\%$  below 2 GHz, increasing to  $\pm 15\%$  above 3 GHz. Sources of uncertainty include instrumental errors (it provides main contribution), sample dimension tolerances, and simulation residuals.

## 5. Conclusions

The frequency range of the single-turn inductor method can be extended into the GHz regime by using electromagnetic simulation software and inverse problem-solving techniques. This provides a significant improvement over traditional analytical models, which are valid only in the lumped-element regime. The use of Ansoft HFSS and optimization techniques enables material parameter extraction even in complex sample geometries and beyond the validity range of simple models.

Compared to earlier methods that rely on closed-form expressions or lumped approximations, our approach allows for accurate characterization across a wider frequency range. This is particularly useful for applications such as high-speed switching devices, RF absorbers, or beam coupling impedance modeling in accelerators, where the behavior

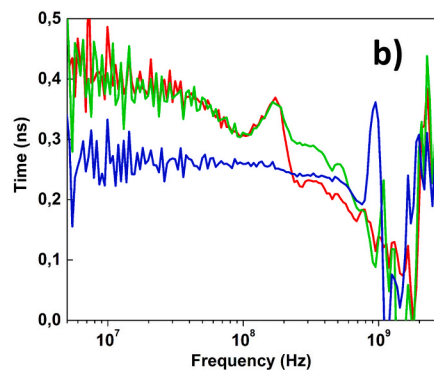


Fig. 7. Measurement setup using microstrip method for AL-800 ferrite a). Group delay dependence on frequency when external field of 5 mT was applied b). Curves colors corresponds to field direction shown in a) picture.

of ferrites must be known over several GHz.

The uncertainty analysis confirms that while numerical methods introduce some variability, the results remain within acceptable ranges for most engineering applications. The microstrip method additionally offers the possibility to measure anisotropic permeability tensors by reorienting the sample or applying external magnetic fields. This opens new opportunities for characterizing advanced magnetic materials used in tunable and directional devices.

### CRedit authorship contribution statement

**Saulius Rudys:** Writing – original draft, Software, Formal analysis, Data curation. **Christine Vollinger:** Writing – original draft, Supervision, Methodology, Investigation, Conceptualization. **Liudas Tumonis:** Software, Methodology, Investigation, Data curation. **Juras Banys:** Writing – review & editing, Writing – original draft, Supervision, Methodology. **Vidmantas Kalendra:** Writing – review & editing, Writing – original draft, Supervision, Project administration.

### Declaration of competing interest

The authors declare the following financial interests/personal relationships which may be considered as potential competing interests: Vidmantas Kalendra reports financial support was provided by Research Council of Lithuania. If there are other authors, they declare that they have no known competing financial interests or personal relationships that could have appeared to influence the work reported in this paper.

### Acknowledgment

This research has been carried out in the framework of the agreement of Vilnius University with the Lithuanian Research Council No. VS-13 and S-CERN-24-3.

### Data availability

Data will be made available on request.

### References

- [1] V.G. Harris, Modern microwave ferrites, *IEEE Trans. Magn.* 48 (3) (Mar. 2012) 1075–1104, <https://doi.org/10.1109/TMAG.2011.2180732>.
- [2] M.J. Barnes, A. Adraktas, G. Bregliozi, B. Goddard, L. Ducimetière, B. Salvant, et al., Operational experience of the upgraded LHC injection kicker magnets during Run 2 and future plans, *J. Phys. Conf. Ser.* 874 (1) (2017) 012101, <https://doi.org/10.1088/1742-6596/874/1/012101>.
- [3] R. Nazlan, M. Hashim, I. Ismail, et al., Compositional and frequency dependent-magnetic and microwave characteristics of indium substituted yttrium iron garnet, *J. Mater. Sci.: Mater. Electron.* 28 (2017) 3029–3041, <https://doi.org/10.1007/s10854-016-5889-z>.
- [4] T. Tsutaoka, T. Kasagi, K. Hatakeyama, Permeability spectra of yttrium iron garnet and its granular composite materials under dc magnetic field, *J. Appl. Phys.* 110 (2011) 053909, <https://doi.org/10.1063/1.3626057>.
- [5] J. Grigas, *Microwave Dielectric Spectroscopy of Ferroelectrics and Related Materials*, Amsterdam, Gordon and Breach, The Netherlands, 1996.
- [6] Š. Švirskas, D. Jablonskas, S. Rudys, S. Lapinskas, R. Grigalaitis, J. Banys, Broad-band measurements of dielectric permittivity in coaxial line using partially filled circular waveguide, *Rev. Sci. Instrum.* 91 (2020) 084703, <https://doi.org/10.1063/1.5136317>.
- [7] J. Banys, S. Lapinskas, S. Rudys, S. Greičius, R. Grigalaitis, High frequency measurements of ferroelectrics and related materials in coaxial line, *Ferroelectrics* 414 (2011) 64–69, <https://doi.org/10.1080/00150193.2011.577308>.
- [8] A.M. Nicolson, G.F. Ross, Measurement of the intrinsic properties of materials by time-domain techniques, *IEEE Trans. Instrum. Meas.* 19 (4) (Nov. 1970) 377–382, <https://doi.org/10.1109/TIM.1970.4313932>.
- [9] W.B. Weir, Automatic measurement of complex dielectric constant and permeability at microwave frequencies, *Proc. IEEE* 62 (1) (Jan. 1974) 33–36, <https://doi.org/10.1109/PROC.1974.9382>.
- [10] T. Tosaka, K. Fujii, K. Fukunaga, A. Kasamatsu, Development of complex relative permittivity measurement system based on free-space in 220–330 GHz range, *IEEE Trans. Terahertz Sci. Technol.* 5 (1) (Jan. 2015) 102–109, <https://doi.org/10.1109/TTHZ.2014.2362013>.
- [11] S. Rudys, M. Ivanov, J. Banys, Ansoft HFSS software application for the dielectric and magnetic measurements of ferroelectrics and related materials in microwaves, *Ferroelectrics* 430 (2012) 115–122, <https://doi.org/10.1080/00150193.2012.677732>.
- [12] D. Jablonskas, S. Lapinskas, S. Rudys, M. Ivanov, J. Banys, Full-wave finite space model of open-ended coaxial line for dielectric spectroscopy of liquids, *Rev. Sci. Instrum.* 88 (8) (2017) 084703, <https://doi.org/10.1063/1.4991312>.
- [13] M.A. Stuchly, S.S. Stuchly, Coaxial line reflection methods for measuring dielectric properties of biological substances at radio and microwave frequencies—A review, *IEEE Trans. Instrum. Meas.* 29 (3) (Sep. 1980) 176–183, <https://doi.org/10.1109/TIM.1980.4314902>.
- [14] J.P. Grant, R.N. Clarke, G.T. Symm, N.M. Spyrou, A critical study of the open-ended coaxial line sensor technique for RF and microwave complex permittivity measurements, *J. Phys. e: Sci. Instrum.* 22 (9) (1989) 757–770, <https://doi.org/10.1088/0022-3735/22/9/015>.
- [15] G. Panariello, L. Verolino, G. Vitolo, Efficient and accurate full-wave analysis of the open-ended coaxial cable, *IEEE Trans. Microw. Theory Techn.* 49 (7) (Jul. 2001) 1304–1309, <https://doi.org/10.1109/22.932251>.
- [16] W.J. Ellison, J.M. Moreau, Open-ended coaxial probe: Model limitations, *IEEE Trans. Instrum. Meas.* 57 (9) (Sep. 2008) 1984–1991, <https://doi.org/10.1109/TIM.2008.917683>.
- [17] R. M. White, *Quantum Theory of Magnetism: Magnetic Properties of Materials*, Berlin, Germany: Springer, 2007, doi: 10.1007/978-3-540-69025-2.
- [18] National Magnetics Group, “National Magnetics Group,” Accessed: Feb. 21, 2025. [Online]. Available: <https://www.magneticsgroup.com/>.
- [19] S. Rudys, S. Balčiūnas, Ch. Vollinger, J. Banys, V. Kalendra, Investigation of dielectric and magnetic properties of AL-800 ferrite, *Lith. J. Phys.* 62 (4) (2022) 277–281, <https://doi.org/10.3952/physics.v62i4.4824>.